# Boehmite Nanofiber–Melamine–Formaldehyde Composite Aerogels and Derivatives for Thermal Insulation and Optical Applications

*Gen Hayase**

Research Center for Materials Nanoarchitectonics, National Institute for Materials Science, 1-1 Namiki, Tsukuba, Ibaraki 305-0044, Japan

ABSTRACT. Machinable composite aerogels combining melamine resin and boehmite nanofibers were successfully prepared using a sol–gel reaction in a mixed solvent of aqueous acetic acid and *N*,*N*-dimethylformamide. The composite aerogel exhibits low thermal conductivity and surface processability, making it a potential thermal insulating material for electronic substrates. Transparent *γ*-alumina aerogels and black alumina-graphite aerogels with designed surface topography were also prepared through computer numerical control (CNC) machining and calcination. These aerogels with precise surface structures are expected to have applications in fields such as optical materials.

KEYWORDS. aerogels, boehmite nanofibers, composites, mechanical properties, thermal insulation, optical properties, CNC milling

Monolithic aerogels have several outstanding physical properties, such as low thermal conductivity and low refractive index.[1,2] They have been used as high-performance lightweight thermal insulators and as materials for physics experiments.[3,4] However, their low bulk density and light weight make them difficult to handle like porous plastic materials, such as urethane foam. As a result, their use has been limited to specialty applications. In aerogel research, the delicate structure of aerogels results in persistent problems related to mechanical strength. Their brittleness makes bulk aerogels difficult to process once produced. Aerogels typically have a porosity greater than 90 % and their microstructure is composed of nanoscale particles. The necks between the particles in aerogels are easily broken[5] by even small impacts, and cracking, chipping and complete collapse occur rapidly during machining. As a result, it has been nearly impossible to produce precise shapes and sizes. However, if aerogel cutting can be realized, monolithic aerogels will have greater flexibility in terms of bulk shape and can be customized for use in specific applications. Aerogels with complex material geometries can be used in a variety of novel applications, such as thermal insulators that adhere to electronic substrates, lenses that take advantage of the low refractive index, and acoustic materials with controlled sound transmission. In recent years, there have been an increasing number of reports of aerogel composites with improved mechanical properties.[6] In contrast, few studies have focused on precision post-processing.

In recent years, there has been a growing trend to use stacked 3D printers to produce aerogels with specific shapes.[7,8] This technology allows the fabrication of materials with complex shapes, such as hollow structures, with a high degree of design freedom. However, there are still many situations, not only in the case of aerogels, where 3D printer modeling lacks processing precision. On the other hand, computer numerical control (CNC) milling can achieve higher accuracy than

3D printing by adjusting the cutting conditions. In fact, CNC micromilling is still preferred over 3D printing for accuracy and cost reasons in the fabrication of microfluidic devices that require high precision.[9] CNC milling also allow faster cutting when processing large bulk samples or curved surface patterns by changing end mills as needed. Therefore, it is important to consider precision machining of aerogels using CNC milling when looking at application development. However, due to the inherent brittleness of aerogels, there have been very few reports on CNC milling processing.

This study investigates high-strength porous materials composed of boehmite nanofibers (BNFs; aluminium hydroxide oxide) incorporated into a polymer that acts as an aerogel backbone, with the goal of producing a post-processable aerogel. Boehmite nanofibers are one-dimensional structures about 4 nm in diameter, produced by hydrothermal synthesis from aluminum isopropoxide, with the fiber length that can be extended to several thousand times its diameter.[10,11] Commercially available BNF sol dispersed in aqueous acetic acid solutions can be used to produce nanofiber-reinforced porous skeletons when composited with resins obtained from acid-catalyzed aqueous sol–gel reactions.[12–14] This reaction significantly improves the mechanical properties of the composites; for example, macroporous polymethylsilsesquioxane composited with BNFs exhibited higher compressive, flexural, torsional, and frictional strengths than its uncomposited counterpart. Those composites have been used to develop water-repellent cell culture substrates because the improved strength allows patterning by milling on the surface.[15] This study extends our previous findings on the macroporous monoliths and reports on our research into precision machinable BNF melamine resin (BM) aerogels with finer microstructure.

Melamine(–formaldehyde) resin is a representative thermoplastic resin, along with phenol–formaldehyde and resorcinol–formaldehyde resins; their use in the fabrication of monolithic porous materials and aerogels has been reported.[16–18] Water-soluble methylolmelamine, the precursor of melamine resin, is industrially available and undergoes gentle polymerization in acidic aqueous solutions. This property is advantageous for compositing with BNF, which is stably dispersed in weakly acidic aqueous solutions, and was used for the preparation of composite aerogels. In this study, melamine resin aerogels were prepared using Nikaresin S-260 (Nippon Carbide Industries Co., Inc., Japan) as a precursor with acetic acid as a catalyst. In a simple aqueous acetic acid solution, the melamine resin undergoes phase separation as soon as it is formed, and its skeletal structure tends to coarsen. To address this issue, the gelation of the melamine resin in an aqueous acetic acid solution with various organic solvents was tested. A 1:1 mixture of 1 M acetic acid solution and *N,N*-dimethylformamide (DMF) was found to be sufficient to suppress phase separation and produce an aerogel with light transmittance (Figure 1a). The preparation of transparent melamine resin aerogels has been reported using a method that involves supercritical drying after a combination of 4 days of gelation treatment and 5 days of solvothermal treatment with trifluoroacetic acid.[19] However, with this method, wet gels are formed within 3 h under ambient pressure and milder conditions, and transparent aerogels can be reproducibly obtained by supercritical drying. Even when BNF (Alumisol-F3000, Kawaken Fine Chemical Co., Japan) with an average length of 3000 μm was added to the starting composition, the mixed sol did not noticeably aggregate and gelled in a fraction of the time (Fig. 1b). After supercritical drying of the organogels, white composite aerogels were successfully obtained. The detailed process for the synthesis of melamine resin/BM aerogels is as follows (Scheme 1). First, $x$ g of methylolmelamine ($x$ = 0.5, 1.0, 1.5) was dissolved in a mixture of 5 mL of aqueous acetic

acid solution containing $y$ % by weight of BNF ($0 \leq y \leq 5.0$) and 5 mL of DMF. The mixture was then incubated in a sealed vessel at 80°C for 24 h. The wet gels were then removed from the vessel and immersed in methanol, 2-propanol and hexane in that order for washing and solvent exchange. Finally, the wet gel was dried by supercritical drying to obtain the final sample "BM$x$-$y$", where $y = 0$ is a pure melamine resin aerogels and the rest are BM composite ones. The process was easily scalable and could produce more than 100 mL of aerogel at a time. However, the compositional range within which defect-free and reproducible BM aerogels could be produced was limited. It was observed that when a small amount of methylolmelamine ($x = 0.5$) was used in the initial composition, the aerogels were prone to uneven shrinkage during drying. On the other hand, when higher amounts of methylolmelamine ($x = 1.5$) were used, the viscosity increased and numerous bubbles developed in the bulk material. At the optimum amount of methylolmelamine ($x = 1.0$), no bubbles remained in the bulk. However, it was difficult to obtain samples without any bubbles on the surface.

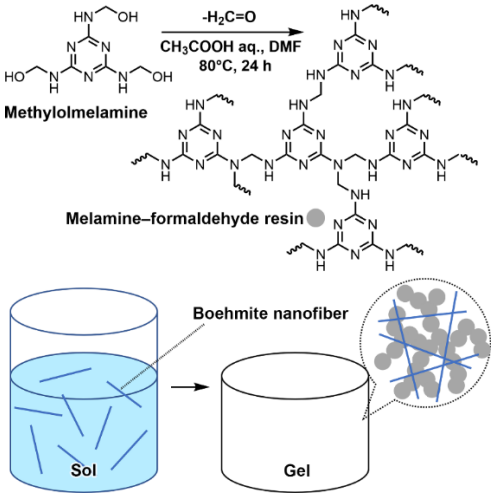


**Scheme 1.** Boehmite nanofiber–melamine–formaldehyde composite aerogels preparation. Monolithic materials were obtained consisting of a microstructure of BNFs interlaced between melamine backbones.

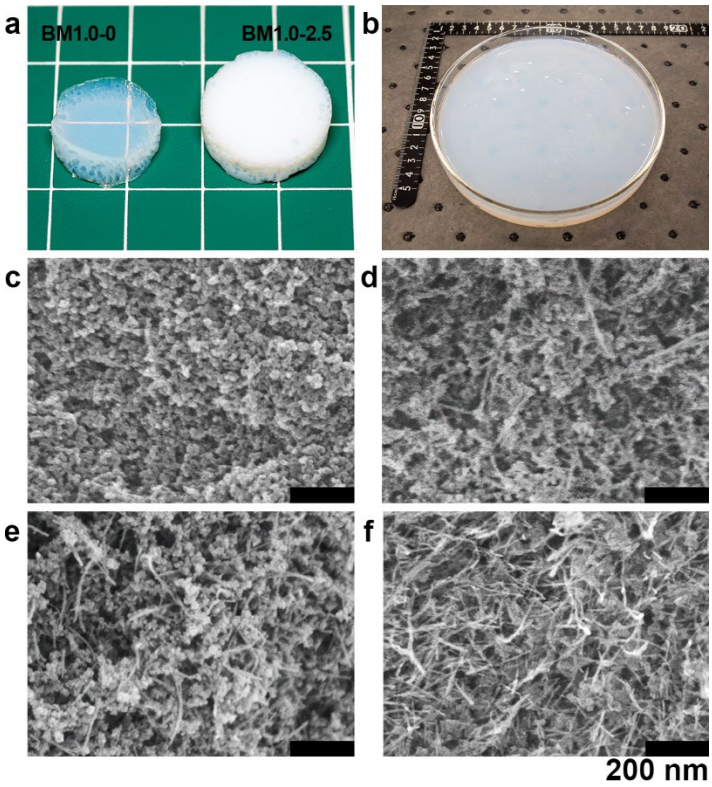


**Figure 1.** (a) Photograph of the light-transmissive melamine resin aerogel and white BM aerogel. (b) Photograph of BM 1.0-2.5 gelled on a 100 mL scale. Scanning electron microscopy (SEM) images of BM *x*-*y*: (c) BM1.0-0, (d) BM1.0-1.0, (e) BM1.0-2.5, (f) BM1.0-5.0.

The addition of nanofibers to composite aerogels can have an impact on the physical properties and processability of the aerogels. Table 1 lists the physical properties of the aerogel samples obtained at different melamine resin quantities and BNF concentrations. It can be observed that the pure melamine resin aerogels, BM*x*-0, experienced shrinkage during the drying process. However, in the composite aerogels containing nanofibers, this shrinkage was found to be suppressed to less than 3 % in terms of length, leading to a decrease in bulk density and Young's modulus. An increase in the BNF concentration resulted in the loss of the continuous structure of the melamine resin aerogel (Figures 1c-f), and the specific surface area decreased accordingly. The FESEM images and infrared spectra (Figure S1) suggest that melamine and BNFs are

physically entangled rather than forming chemical bonds. The pure melamine resin aerogel BM1.0-0 was found to be prone to nonuniform shrinkage when its fabrication scale was increased, which can lead to the loss of porosity and a decrease in performance such as visible light transmission and mechanical strength against impact. In contrast, the composite aerogel was obtained with good reproducibility, suggesting that the addition of BNFs can help stabilize the aerogel structure during drying and prevent nonuniform shrinkage. Boehmite nanofiber-melamine resin composite aerogels exhibited elasticity (Figure S2) and were clearly more resistant to chipping and abrasion than silica aerogels. The thermal conductivity of the composite aerogels was measured by the heat flowmeter method and showed a minimum value of 0.0214 W $m^{-1}$ $K^{-1}$ for BM 1.0-2.5, which is below the thermal conductivity of room temperature air of 0.026 W $m^{-1}$ $K^{-1}$. Moreover, this thermal conductivity value was intermediate between those of alumina aerogel (0.029 W $m^{-1}$ $K^{-1}$, measured by guarded hot plate method)[20] and melamine aerogel (0.013 W $m^{-1}$ $K^{-1}$, measured by a transient method). The difference in thermal conductivity between samples can be explained by solid phase heat transfer: increase in bulk density due to drying shrinkage in BM 1.0-1.0 and increase in BNF amount with higher thermal conductivity in BM 1.0-5.0.[21]

As a result of the improved mechanical properties resulting from compositing, it was possible to engrave letters and fabricate arbitrary concave and convex shapes on the surface of BM1.0-$x$ ($x$ =1.0, 2.5, and 5.0) aerogels by using a CNC milling machine (Figure 2). The ability to machine the surface of BM1.0-2.5 to form square pillars with a length of 0.5 mm without difficulty promotes the application of the composite aerogel as a heat insulating material for electronic substrates with uneven surfaces.

**Table 1.** Physical properties of the melamine resin/composite aerogels BM*x*-*y* and BNFs.

| Sample | Density [g $cm^{-3}$] | Young's modulus [MPa] | BET surface area [$m^2$ $g^{-1}$] | Thermal conductivity [W $m^{-1}$ $K^{-1}$] |
|---|---|---|---|---|
| BM 0.5-0 | 0.273 | 4.16 | 576 | - |
| BM1.0-0 | 0.287 | 7.94 | 626 | - |
| BM1.0-1.0 | 0.158 | 2.73 | 589 | 0.0240 |
| BM1.0-2.5 | 0.139 | 2.57 | 561 | 0.0214 |
| BM1.0-5.0 | 0.136 | 0.696 | 389 | 0.0267 |
| BM1.5-0 | 0.263 | 10.2 | 649 | - |
| BNF | - | - | 380 | - |

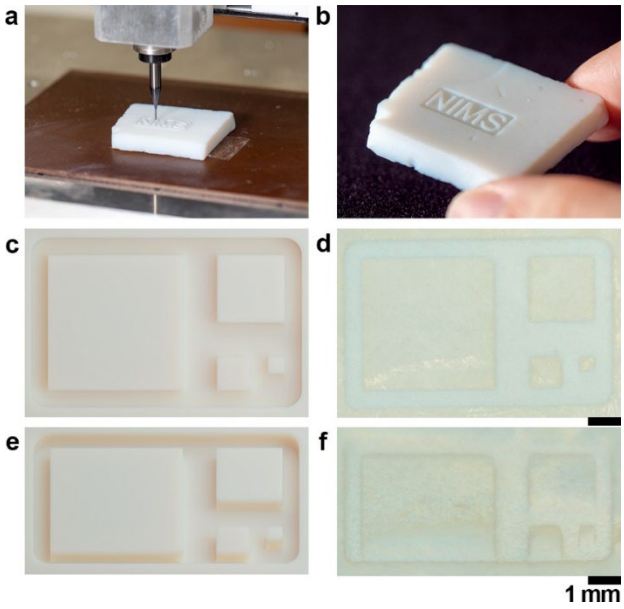

**Figure 2.** Photographs of (a) BM1.0-2.5 subjected to CNC milling and (b) the machined sample. (c) Computer graphics produced from CAD data used for CNC milling and (d) digital microscope image of an actual sample of BM1.0-2.5. The depth of cut is 0.5 mm. (e,f) Tilt-observation computer graphic/actual images of (c) and (d), respectively.

Some researchers have reported the preparation of monolithic porous materials by using melamine resin as a mold or support material and firing it under oxidizing conditions.[22–24] Removal of melamine resin from the composite aerogel results in a loss of thermal insulation properties due to the large pore size expansion, while optical properties can be expected by taking advantage of the nanofiber structure. I attempted to fabricate light-transmissive γ-alumina aerogels with designed surface morphology by oxidizing and removing the melamine portion of surface-shaped BM aerogels at 500 °C. Among the BM composites, the calcined BM1.0-1.0 and BM1.0-2.5 aerogels underwent significant shrinkage and collapse of their shape (Figure S3). This shrinkage may be due to the low density of the nanofibers and their inability to provide adequate support during the pyrolysis of the melamine resin. However, BM1.0-5.0 was heat treated in air and transformed to a transparent alumina aerogel with almost no shrinkage, retaining their shape after heat treatment in the air, as shown in Figures 3c-e. We have previously reported that pure BNF aerogels shrink very little after heat treatment at 600°C.[25] It is likely that the presence of a certain amount of BNFs prevented shrinkage in this study as well. The transparent aerogel transmitted 79.2% of visible light at a wavelength of 550 nm at a thickness of 5 mm (Figure S4). In a previous study, pure BNF aerogels were obtained through the supercritical drying of a BNF sol after gelation with a base or phosphoric acid;[25,26] however, it was challenging to directly process the surfaces of these nanofiber structures. Processing strength was significantly enhanced once composited with the melamine resin, allowing the design of

transparent aerogels. The calcination of BM1.0-5.0 in a nitrogen atmosphere yielded black aerogels, while maintaining their bulk shape (Figures 3f-h). Bulk density analysis, SEM (Figure 3e-f), energy dispersive X-ray spectroscopy (Figure S5), and micro-Raman spectroscopy (Figure S6) results suggest that during pyrolysis, the melamine resin adhered to the surface of graphite while bundling alumina nanofibers. The structure exhibited a reflectance of <0.7% at visible light wavelengths (Figure S7). Carbon aerogels obtained by calcination of resorcinol–formaldehyde aerogels in an inert atmosphere have been reported to exhibit high absorption rates because the incident light is efficiently absorbed, while being reflected through porous media.[27,28] It is considered that light confinement may occur in a similar manner in the alumina–graphite aerogels. The Young's modulus for both transparent and black aerogels was about 300 kPa. However, there was an error of several tens of percent in the values. The key to the fabrication of these optical aerogels was the rate of temperature increase. The temperature increase rate must be constant at 100 °C $h^{-1}$ (or much slower; the operating program is shown in Figure S8, Supporting Information) because aerogels tend to shrink if the temperature is increased rapidly. This should allow the aerogel to heat uniformly from the surface to the interior and slowly release the generated gases. To the best of our knowledge, no studies have reported similar findings on aerogels, especially with the ability to accurately process the aerogel surfaces using a CNC milling machine. Aerogels have been utilized as optical materials in various physical experiments,[29,30] and we anticipate that their application scope can be further expanded through the implementation of surface processing techniques. Currently, the compositional conditions for the fabrication of thermally processable aerogels are within a narrow range. However, optimization of the polymerization conditions of the melamine resin and the aspect ratio of the nanofibers is expected to improve the ease of fabrication.

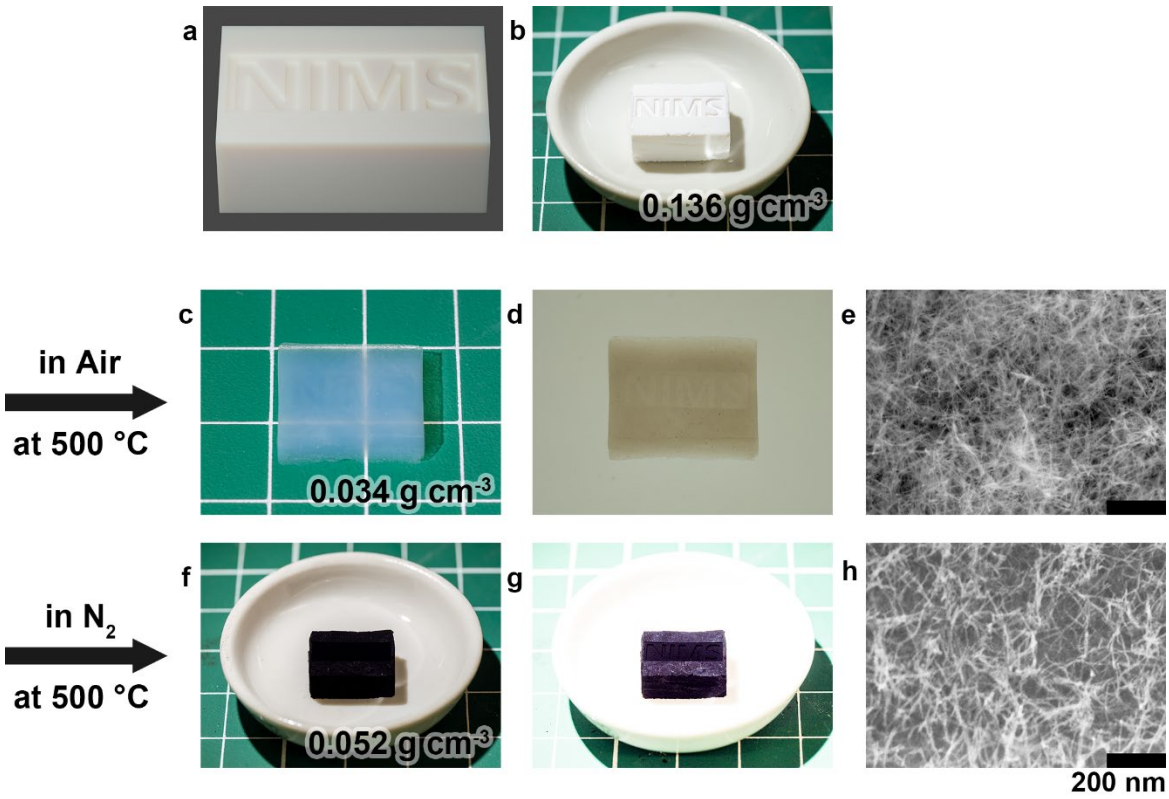


**Figure 3.** (a) Computer graphic produced from CAD data used for CNC milling, (b) Photograph of actual BM 1.0-5.0. The letters "NIMS" are engraved on the sample surface at a depth of 0.2 mm. The background grid spacing is 10 mm. (c) Photograph of the transparent alumina aerogels obtained by heat treatment in air. (d) Photograph of the same sample as (c) taken on an LED board. (e) SEM image of the transparent alumina aerogel. (g, f) Photograph of black alumina-graphite aerogel obtained in $N_2$; the two photographs were generated from the same data at different brightness levels to make the appearance and surface conditions easier to see. (h) SEM image of the black alumina-graphite aerogel.

In summary, CNC-machinable composite aerogels were successfully prepared using the melamine resin and BNFs. A mixture of aqueous acetic acid and DMF was used to prepare the melamine resin gel from methylolmelamine, allowing the reaction to expedite the fabrication process. The addition of BNFs to this mixed solution did not cause any significant agglomeration

in the resulting gel, thereby facilitating the complexation process. The physical properties and processability of the obtained BM composite aerogels were investigated. The addition of BNFs to the melamine resin enhanced the physical properties of the aerogel because of the suppression of shrinkage during gelation and supercritical drying, resulting in a decrease in the bulk density and Young's modulus. The BM composite aerogels, possessing low thermal conductivity (0.0214 W $m^{-1}$ $K^{-1}$) and the surface processability with sub-millimeter accuracy, have a potential application as a thermal insulating material for electronic substrates. Additionally, transparent γ-alumina aerogels with an intact surface design were produced by heating the surface-processed BM aerogel to 500 °C in air to remove the melamine components. Calcination of the same BM aerogel in a nitrogen atmosphere produced alumina-graphite aerogels with high light absorption as well. The successful fabrication of aerogels with designed surface topography and optical features was attributed to the low heating rate, which minimized aerogel shrinkage and preserved the nanofiber structure. The aerogels with precise surface morphology obtained by CNC machining and appropriate thermal treatment in this study are expected to have applications in optical materials and other fields.

## ASSOCIATED CONTENT

**Supporting Information**.

The following files are available free of charge.

Experimental details, infrared spectra, compressive stress-strain curves, photographs of black alumina-graphite aerogels, transmittance spectra of *γ*-alumina aerogel, EDX measurement data, micro-Raman spectra, reflectance spectra, heat treatment program (PDF)

## AUTHOR INFORMATION

**Corresponding Author**

* Email: gen@aerogel.jp

**Notes**

The author declares no conflicts of interest.

ACKNOWLEDGMENT

This research was supported by MEXT Leading Initiative for Excellent Young Researchers (LEADER) program. Research Center for Materials Nanoarchitectonics (MANA) is supported by World Premier International Research Center Initiative (WPI), MEXT, Japan. I would like to express my gratitude to Dr. Gaku Imamura for his assistance with the micro-Raman measurements, and to Dr. Mizuki Tenjimbayashi for her help with the digital optical microscope observations.

REFERENCES

(1) Fricke, J.; Tillotson, T. Aerogels: Production, Characterization, and Applications. *Thin Solid Films* **1997**, *297* (1), 212–223. https://doi.org/10.1016/S0040-6090(96)09441-2.

(2) Pierre, A. C.; Pajonk, G. M. Chemistry of Aerogels and Their Applications. *Chem. Rev.* **2002**, *102* (11), 4243–4265. https://doi.org/10.1021/cr0101306.

(3) Sumiyoshi, T.; Adachi, I.; Enomoto, R.; Iijima, T.; Suda, R.; Yokoyama, M.; Yokogawa, H. Silica Aerogels in High Energy Physics. *J. Non-Cryst. Solids* **1998**, *225*, 369–374. https://doi.org/10.1016/S0022-3093(98)00057-X.

(4) Smith, D. M.; Maskara, A.; Boes, U. Aerogel-Based Thermal Insulation. *J. Non-Cryst. Solids* **1998**, *225*, 254–259. https://doi.org/10.1016/S0022-3093(98)00125-2.

(5) Hæreid, S.; Anderson, J.; Einarsrud, M. A.; Hua, D. W.; Smith, D. M. Thermal and Temporal Aging of TMOS-Based Aerogel Precursors in Water. *J. Non-Cryst. Solids* **1995**, *185* (3), 221–226. https://doi.org/10.1016/0022-3093(95)00016-X.

(6) Maleki, H.; Durães, L.; Portugal, A. An Overview on Silica Aerogels Synthesis and Different Mechanical Reinforcing Strategies. *J. Non-Cryst. Solids* **2014**, *385*, 55–74. https://doi.org/10.1016/j.jnoncrysol.2013.10.017.

(7) Zhao, S.; Siqueira, G.; Drdova, S.; Norris, D.; Ubert, C.; Bonnin, A.; Galmarini, S.; Ganobjak, M.; Pan, Z.; Brunner, S.; Nyström, G.; Wang, J.; Koebel, M. M.; Malfait, W. J. Additive Manufacturing of Silica Aerogels. *Nature* **2020**, *584* (7821), 387–392. https://doi.org/10.1038/s41586-020-2594-0.

(8) Zou, W.; Wang, Z.; Qian, Z.; Xu, J.; Zhao, N. Digital Light Processing 3D-Printed Silica Aerogel and as a Versatile Host Framework for High-Performance Functional Nanocomposites. *Adv. Sci.* **2022**, e2204906. https://doi.org/10.1002/advs.202204906.

(9) Guckenberger, D. J.; de Groot, T. E.; Wan, A. M. D.; Beebe, D. J.; Young, E. W. K. Micromilling: A Method for Ultra-Rapid Prototyping of Plastic Microfluidic Devices. *Lab Chip* **2015**, *15* (11), 2364–2378. https://doi.org/10.1039/c5lc00234f.

(10) Nagai, N.; Mizukami, F. Properties of Boehmite and Al2O3 Thin Films Prepared from Boehmite Nanofibres. *J. Mater. Chem.* **2011**, *21* (38), 14884–14889. https://doi.org/10.1039/C1JM11571E.

(11) Iijima, S.; Yumura, T.; Liu, Z. One-Dimensional Nanowires of Pseudoboehmite (Aluminum Oxyhydroxide γ-AlOOH). *Proc. Natl. Acad. Sci. U. S. A.* **2016**, *113* (42), 11759–11764. https://doi.org/10.1073/pnas.1614059113.

(12) Hayase, G.; Nonomura, K.; Kanamori, K.; Maeno, A.; Kaji, H.; Nakanishi, K. Boehmite Nanofiber–Polymethylsilsesquioxane Core–Shell Porous Monoliths for a Thermal Insulator under Low Vacuum Conditions. *Chem. Mater.* **2016**, *28* (10), 3237–3240. https://doi.org/10.1021/acs.chemmater.6b01010.

(13) Hayase, G. Fabrication of Boehmite Nanofiber Internally-Reinforced Resorcinol-Formaldehyde Macroporous Monoliths for Heat/Flame Protection. *ACS Appl. Nano Mater.* **2018**, *1* (11), 5989–5993. https://doi.org/10.1021/acsanm.8b01518.

(14) Hayase, G. Boehmite Nanofiber–Polymethylsilsesquioxane Composite Aerogels: Synthesis, Analysis, and Thermal Conductivity Control via Compression Processing. *Bull. Chem. Soc. Jpn.* **2021**, *94* (1), 70–75. https://doi.org/10.1246/bcsj.20200205.

(15) Hayase, G.; Yoshino, D. CNC-Milled Superhydrophobic Macroporous Monoliths for 3D Cell Culture. *ACS Appl. Bio Mater.* **2020**, *3* (8), 4747–4750. https://doi.org/10.1021/acsabm.0c00719.

(16) Pekala, R. W.; Alviso, C. T.; Kong, F. M.; Hulsey, S. S. Aerogels Derived from Multifunctional Organic Monomers. *J. Non-Cryst. Solids* **1992**, *145*, 90–98. https://doi.org/10.1016/S0022-3093(05)80436-3.

(17) Nguyen, M. H.; Dao, L. H. Effects of Processing Variable on Melamine–Formaldehyde Aerogel Formation. *J. Non-Cryst. Solids* **1998**, *225*, 51–57. https://doi.org/10.1016/S0022-3093(98)00008-8.

(18) Ren, H.; Zhu, J.; Bi, Y.; Xu, Y.; Zhang, L.; Shang, C. Rapid Fabrication of Low Density Melamine–Formaldehyde Aerogels. *J. Porous Mater.* **2018**, *25* (2), 351–358. https://doi.org/10.1007/s10934-017-0446-6.

(19) Nakanishi, Y.; Hara, Y.; Sakuma, W.; Saito, T.; Nakanishi, K.; Kanamori, K. Colorless Transparent Melamine–Formaldehyde Aerogels for Thermal Insulation. *ACS Appl. Nano Mater.* **2020**, *3* (1), 49–54. https://doi.org/10.1021/acsanm.9b02275.

(20) Poco, J. F.; Satcher, J. H.; Hrubesh, L. W. Synthesis of High Porosity, Monolithic Alumina Aerogels. *J. Non-Cryst. Solids* **2001**, *285* (1), 57–63. https://doi.org/10.1016/S0022-3093(01)00432-X.

(21) Hrubesh, L. W.; Pekala, R. W. Thermal Properties of Organic and Inorganic Aerogels. *J. Mater. Res.* **1994**, *9* (3), 731–738. https://doi.org/10.1557/JMR.1994.0731.

(22) Zhu, G.; Xi, C.; Liu, Y.; Zhu, J.; Shen, X. CN Foam Loaded with Few-Layer Graphene Nanosheets for High-Performance Supercapacitor Electrodes. *J. Mater. Chem. A* **2015**, *3* (14), 7591–7599. https://doi.org/10.1039/C5TA00837A.

(23) Jiang, B.; He, C.; Zhao, N.; Nash, P.; Shi, C.; Wang, Z. Ultralight Metal Foams. *Sci. Rep.* **2015**, *5*, 13825. https://doi.org/10.1038/srep13825.

(24) Xue, F.; Lu, Y.; Qi, X.-D.; Yang, J.-H.; Wang, Y. Melamine Foam-Templated Graphene Nanoplatelet Framework toward Phase Change Materials with Multiple Energy Conversion Abilities. *Chem. Eng. J.* **2019**, *365*, 20‑29. https://doi.org/10.1016/j.cej.2019.02.023.

(25) Hayase, G.; Nonomura, K.; Hasegawa, G.; Kanamori, K.; Nakanishi, K. Ultralow-Density, Transparent, Superamphiphobic Boehmite Nanofiber Aerogels and Their Alumina Derivatives. *Chem. Mater.* **2015**, *27* (1), 3–5. https://doi.org/10.1021/cm503993n.

(26) Hayase, G.; Yamazaki, K.; Kodaira, T. Fabrication of Boehmite Nanofiber Aerogels by a Phosphate Gelation Process for Optical Applications. *J. Sol-Gel Sci. Technol.* **2022**, *104* (3), 558–565. https://doi.org/10.1007/s10971-022-05867-0.

(27) Merzbacher, C. I.; Meier, S. R.; Pierce, J. R.; Korwin, M. L. Carbon Aerogels as Broadband Non-Reflective Materials. *J. Non-Cryst. Solids* **2001**, *285* (1), 210–215. https://doi.org/10.1016/S0022-3093(01)00455-0.

(28) Sun, W.; Du, A.; Feng, Y.; Shen, J.; Huang, S.; Tang, J.; Zhou, B. Super Black Material from Low-Density Carbon Aerogels with Subwavelength Structures. *ACS Nano* **2016**, *10* (10), 9123–9128. https://doi.org/10.1021/acsnano.6b02039.

(29) Hotaling, S. P. Ultra-Low Density Aerogel Optical Applications. *J. Mater. Res.* **1993**, *8* (2), 352–355. https://doi.org/10.1557/JMR.1993.0352.

(30) Poelz, G.; Riethmüller, R. Preparation of Silica Aerogel for Cherenkov Counters. *Nucl. Instrum. Methods Phys. Res.* **1982**, *195* (3), 491–503. https://doi.org/10.1016/0029-554X(82)90010-6.

ToC